Spectrochimica Acta Part A: Molecular and Biomolecular Spectroscopy 204 (2018) 777–782

Contents lists available at ScienceDirect

Spectrochimica Acta Part A: Molecular and Biomolecular Spectroscopy

journal homepage: www.elsevier.com/locate/saa

A targetable fluorescent probe for real-time monitoring of fluoride ions in mitochondria

Kai Zhou, Mingguang Ren, Li Wang, Zihong Li, Weiying Lin *

Institute of Fluorescent Probes for Biological Imaging, School of Chemistry and Chemical Engineering, School of Materials Science and Engineering, University of Jinan, Jinan, Shandong 250022, PR China

ARTICLE INFO

Article history:
Received 28 March 2018
Received in revised form 6 May 2018
Accepted 15 May 2018
Available online xxxx

Keywords:
Fluorescent probe
Mitochondria
Fluoride ions
Fluorescence imaging

ABSTRACT

Fluorion are pivotal anions in biology because they play an important role in dental care, treating osteoporosis, preventing tooth decay and promoting the healthy growth of bone. Studies have shown that high levels of fluoride will lead to the inactivation of the mitochondria. Therefore, it is urgent to develop a method to detect the fluoride anions in the mitochondria. Herein, we have developed a novel mitochondrial-target fluorescent probe for detecting F^- in living cells. The probe exhibited excellent sensitivity and high selectivity for F^- over the other relative species. With changing fluoride ions, the fluorescence spectrum of the probe changed significantly with a large turn-on fluorescence signal. Cell imaging indicated that the probe can penetrate viable cell membranes and rapidly detects and images fluorion over other anions in the mitochondria.

1. Introduction

Fluoride ions, the smallest and most negative anions, are of particular interest due to their important role in dental care and promoting the healthy growth of bone [1–3]. However, excessive fluoride can cause various diseases such as, metabolic disturbances, tooth mottling, skeletal fluorosis, immune damage, neurotoxicity, and kidney disease [4,5]. Additionally, NaF, as an effective activator of G protein and inhibitor for Ser/Thr phosphatase, affects plenty of essential cell signaling elements [6]. At the cell organelles level, studies have shown that high levels of fluoride can cause oxidative stress on mitochondria and reduce mitochondrial respiratory chain efficiency, and leading to mitochondrial dysfunction, which is an earliest event in most delayed neurodegenerative diseases [7–10]. In order to fully elucidate the toxicity of fluoride ions, it is very necessary to develop a sensitive, specific and accurate method for the detection of its distribution and dynamic fluctuation in biological systems. For traditional methods, including ^{19}F NMR spectroscopy [11], ion chromatography [12] and ion-selective electrodes [13], complicated pre-treatments of samples, relatively cumbersome equipment, and professional operators are require ineluctably, which hinders their application in the effective and convenient detection of F^-. In the various analytical methods available, fluorescence sensing is regarded as an ideal technology due to its advantages of simplicity of operation, high specificity and sensitivity [14–19]. Although significant progresses have been made in the development of plenty fluorescent fluoride ions probes [20–26], there are still some deficiencies in practical applications. For example, some B-F complexing sensors are often sensitive to oxygen and moisture and involve complex equilibria due to the formation of various fluoroborate species. Furthermore, some desilylation F^- probes usually require an excess of F ions to reach saturation and the response time required is often longer. Currently, fluorescent F^- probes based on H-bond interaction are more fascinating due to their satisfactory response time and stable chemical property. Although several fluoride ion fluorescence sensors based on F-induced deprotonation through H-bonding with protonic units have been reported [27–31], rare of them can be used for the detection and imaging of fluorinion levels in cellular mitochondria.

Herein, we designed and synthesized a new intramolecular charge transfer (ICT) based, mitochondrial-targeted fluorescent probe (**Mito-FV**) by linking imidazole (donor, D) and hemicyanine (acceptor, A) through a phenyl ring. The sensor **Mito-FV** exhibited excellent sensitivity and high selectivity for F^- over the other relative species and can display strong turn-on (~204-fold) fluorescence in response to F^-. Furthermore, **Mito-FV** was able to penetrate the membranes of living cells, rapidly detect and image the F^- in mitochondria.

2. Experimental

2.1. Materials and Instruments

Unless otherwise noted, all reagents were obtained from commercial suppliers, and used directly without further purification. Solvents used in experiment were purified by standard methods prior to use. The water used in all experiments refers to the twice-distilled water.

* Corresponding author.
E-mail address: weiyinglin2013@163.com (W. Lin).

https://doi.org/10.1016/j.saa.2018.05.054
1386-1425/

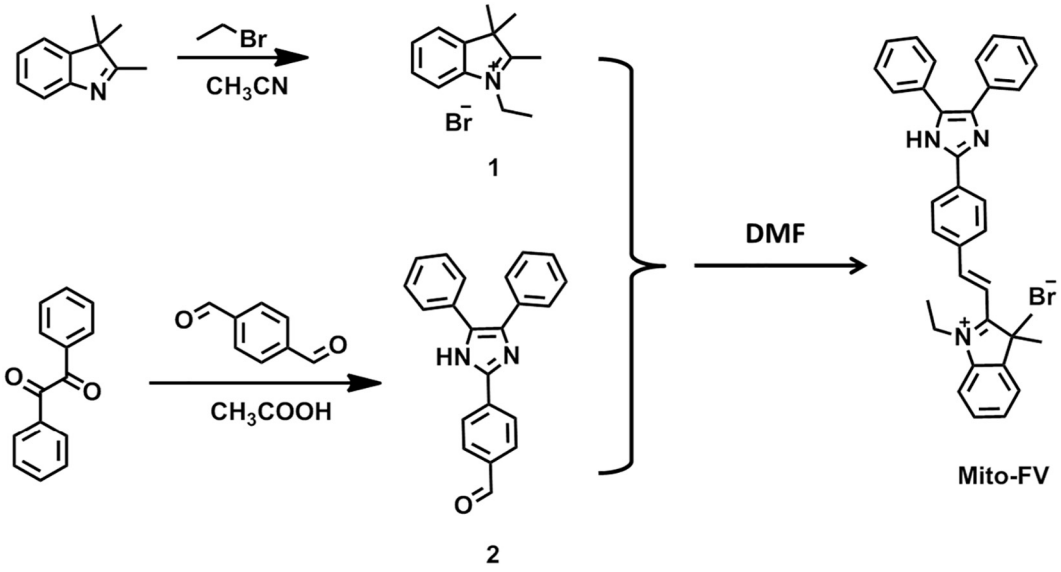

Scheme 1. Synthesis route of probe **Mito-FV**.

The instruments used in this work were same as those in our previously reported articles [32].

2.2. Synthesis of *Mito-FV*

The synthesis route of **Mito-FV** was outlined in Scheme 1. Compound **1** and **2** were prepared referencing the reported literature [33,34]. The desired compound **Mito-FV** was readily obtained in one simple step. Dissolved the crude product **1** (200 mg, 0.75 mmol, 1.0 eq) and compound **2** (245 mg, 0.75 mmol, 1.0 eq) in 4 mL *N*,*N*-dimethylformide (DMF), and the mixture was refluxed for 6 h at 90 °C under a nitrogen atmosphere. After cooled to room temperature, the mixture was poured into water and extracted with dichloromethane. Subsequently, the organic layer was combined, washed with water and brine, dried over sodium sulfate, filtered, and then concentrated in vacuo. The residue was purified by column chromatography on silica gel (petroleum ether to MeOH/DCM = 1/20, v/v) to afford the target compound **Mito-FV** (210 mg purple powder, yield: 48%). ^{1}H NMR (400 MHz, DMSO) δ 13.34 (s, 1H), 8.53 (d, J = 16.2 Hz, 1H), 8.42 (d, J = 8.9 Hz, 2H), 8.39 (d, J = 8.8 Hz, 2H), 7.98 (dd, J = 5.2, 3.7 Hz, 1H), 7.94–7.90 (m, 1H), 7.82 (d, J = 16.3 Hz, 1H), 7.67–7.62 (m, 2H), 7.60–7.58 (m, 2H), 7.58–7.55 (m, 2H), 7.46 (t, J = 7.3 Hz, 2H), 7.41 (d, J = 7.2 Hz, 1H), 7.34 (t, J = 7.4 Hz, 2H), 7.26 (t, J = 7.3 Hz, 1H), 4.81 (q, J = 6.9 Hz, 2H), 1.84 (s, 6H), 1.48 (t, J = 7.2 Hz, 3H)·^{13}C NMR (101 MHz, DMSO) δ 181.74 (s), 153.81 (s), 144.94 (s), 144.51 (s), 140.91 (s), 138.91 (s), 135.37 (s), 134.83 (s), 134.42 (s), 131.90 (s), 131.06 (s), 130.29 (s), 129.90 (s), 129.62 (s), 129.09 (d, J = 6.3 Hz), 128.73 (s), 128.52 (s), 127.75 (s), 127.32 (s), 126.02 (s), 123.61 (s), 115.65 (s), 112.64 (s), 52.75 (s), 42.72 (s), 26.09 (s), 14.35 (s). HRMS (ESI): m/z calculated for $C_{35}H_{32}N_3^+$ 494.2591 $[M]^+$, found: 494.2592 (Scheme 2).

3. Results and Discussion

3.1. Design and Synthesis of *Mito-FV*

Imidazole derivatives were wildly applied in different areas due to their favorable properties such as high stability, flexible photophysical properties, high extinction coefficients, and ease synthesis [35–37]. Considering its susceptible to detect anions either by deprotonation of potential —NH fragment or H-bonding interaction, imidazole was selected as the recognition site for F^-. Hemicyanine, as a strong electron withdraw group, was widely applied to the synthesis of dyes and fluorescent probes [38–41]. Moreover, hemicyanine can act as a mitochondrial targeting group and rapidly enter the mitochondria in cells in a short time [42]. Thus, we constructed a mitochondra-target fluorescent probe **Mito-FV** by linking carbazole and hemicyanine through the benzene ring. The target sensor **Mito-FV** was readily synthesized in one simple step. Treatment of compound **1** with the compound **2** in *N*,*N*-dimethylformide afforded probe **Mito-FV** in good yield. The synthesis route of **Mito-FV** was shown in Scheme 1, and the structure was fully characterized by standard ^{1}H NMR, ^{13}C NMR and mass spectrometry in Supporting information.

3.2. Optical Response of *Mito-FV* to F^-

With the probe **Mito-FV** in hand, we initially investigated its optical responses to fluoride ions (TBAF as F^- donor) by absorption and

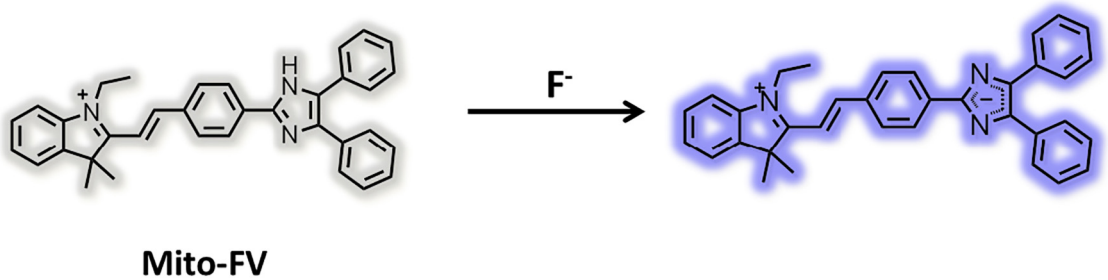

Scheme 2. Proposed response mechanism of **Mito-FV** to F^-.

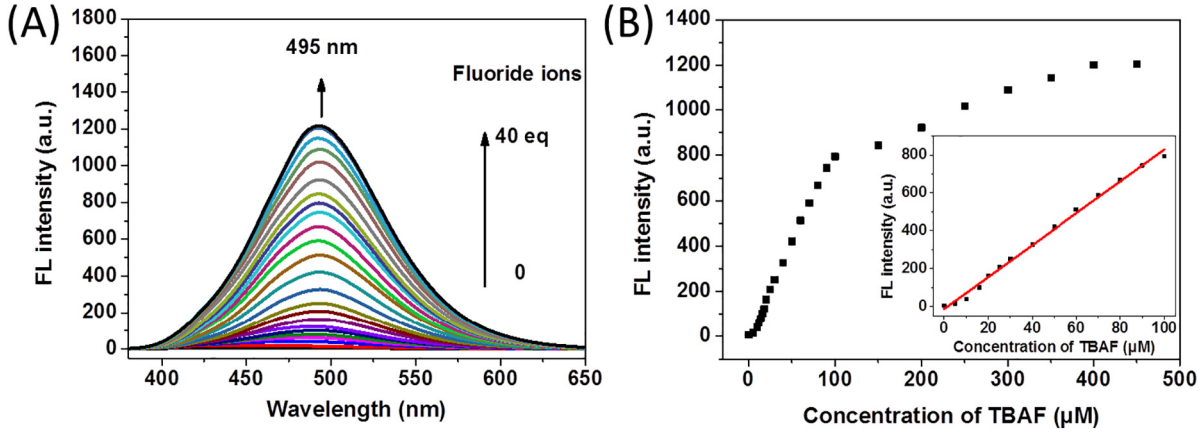

Fig. 1. (A) Fluorescence spectra of **Mito-FV** (10 μM) upon the addition of TBAF (0–40 eq) in CH_3CN after 30 min at room temperature. (B) Fluorescence intensity at 495 nm as a function of F^- concentration. Inset: Linearity between the fluorescence intensity at 495 nm and TBAF concentration in the range of 0–100 μM. (λ_{ex} = 370 nm; EX Slit: 5.0 nm; EM Slit: 5.0 nm; PMT Voltage: 400 V).

emission spectroscopy. Firstly, we studied the absorption spectra of the probe **Mito-FV** with changing the concentration of fluoride ions. As shown in Fig. S1, the free sensor **Mito-FV** displayed two major absorption band at 554 nm and 313 nm. However, with the addition of F^-, the absorption at 554 nm was decreased and the band at 313 nm was increased with a 19 nm red-shift while there is a distinct isosbestic point at 375 nm. An evident naked-eye color changes for the **Mito-FV** solution treated with TBAF was observed from light brown to colorless under ambient light and the fluorescence emission was changed from colorless to bright blue under a UV lamp at 365 nm (Fig. S2). These results mentioned above indicated that **Mito-FV** can serve as a colorimetric detector for the visual detection of fluoride ions.

Subsequently, we studied the emission spectral of **Mito-FV** with the addition of TBAF. As shown in Fig. 1A, **Mito-FV** exhibits weak emission (φ = 0.0043) when excited at 370 nm in CH_3CN. However, upon gradual addition of F^-, the corresponding emission intensity of **Mito-FV** was enhanced accompanied a red-shift and the maximum emission wavelength was shift to 495 nm with the concentration of F^- increased to 10 μM. With the continued addition of fluoride, the corresponding emission intensity of **Mito-FV** enhanced significantly and showed a quantum yield of 0.2797, approximately 65-fold enhancement of the quantum yield with 40 eq of fluoride added, meanwhile, the fluorescence intensity at 495 nm was increased about 204-fold. A good linear correlation (R^2 = 0.99) existed between the fluorescence intensity and the concentration of TBAF within the range from 0 to 100 μM (Fig. 1B), indicating that the probe **Mito-FV** can be utilized for the quantitative determination of fluoride ions.

As there is a decrease at 554 nm in the absorption spectrum, so we chose a long wavelength (530 nm) to excite the probe, induced a weak fluorescence at 717 nm and found a little decrease of the intensity in the presence of a small amount of F^-. However, the fluorescence intensity was plotted as a function of the F^- concentration with a good fitting coefficient for 0.98 (Fig. S4).

On account of the complexity of the intracellular environment, we chose some of the tetrabutylammonium (TBA) salts as the reference to carry out a controlled trial in acetonitrile. The probe **Mito-FV** was treated with various analytes such as NO_3^-, $H_2PO_4^-$, OAc^-, HSO_4^-, I^-, Br^- and Cl^- from TBA salts respectively. As shown in Fig. 2, none but F^- can efficiently exhibit fluorescence emission and the fluorescence intensity of **Mito-FV** in the presence of F^- achieved about 26.5 times than that of other anions. **Mito-FV** showed a strong response toward F^- and negligible responses toward other anions. As seen in Fig. 2A, the spectrum of **Mito-FV** was more susceptible to F^- than these tetrabutyl salts. Therefore, **Mito-FV** seems to be useful for the selective detection of F^- even with these relevant analytes.

The kinetic profiles of the probe **Mito-FV** (10 μM) treated with the varied concentrations of F^- (0, 10 eq, 20 eq, 40 eq) were shown in Fig. 3. The probe **Mito-FV** untreated with F^- had almost no change in the fluorescence intensity at 495 nm. However, a fluorescence enhancement was observed when incubated with F^-, and the signal reached an

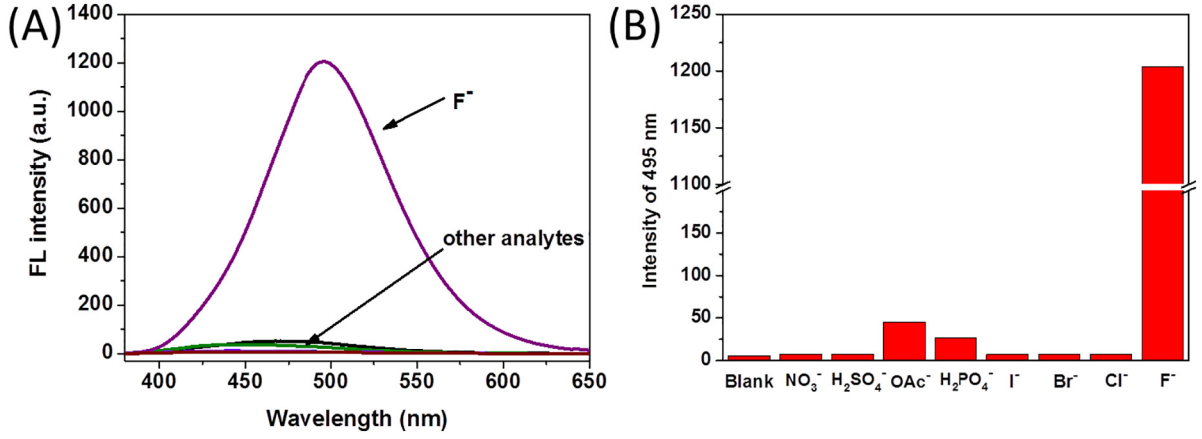

Fig. 2. (A) Fluorescence spectra and (B) fluorescence intensity at 495 nm of **Mito-FV** (10 μM) treated with various species in CH_3CN solution after 30 min at room temperature (Concentration: TBAF, 100 μM; the other species: 200 μM).

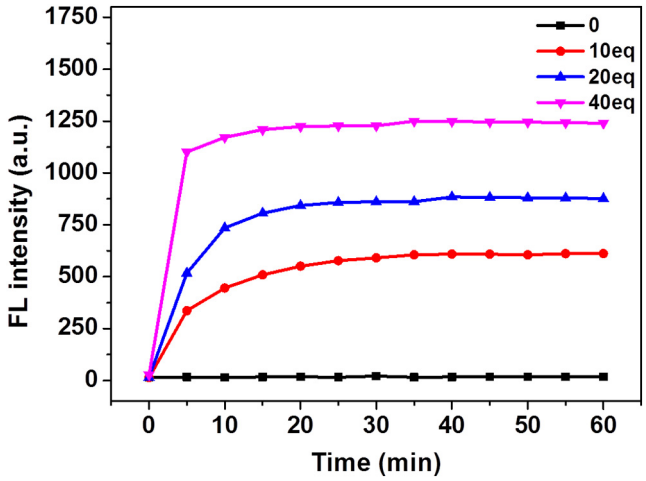

Fig. 3. The fluorescence intensities at 495 nm of **Mito-FV** (10 μM) as a function of time upon addition of different concentration of TBAF (20, 100, 200, 400 μM) at room temperature for continuously monitored in CH_3CN with the excitation at 370 nm.

equilibrium state after about 5–10 min. This superior performance of **Mito-FV** indicated that it may be used as a real-time indicator for F^- detection.

Photostability is one of the most important parameters of fluorescent dyes and probes. Hence, we investigated the photostability of the compound **Mito-FV** under UV light conditions (Fig. S5). Photostability studies suggested that the probe was highly stable, even under excitation using a short wavelength of UV light for 60 min.

3.3. Fluorescence Imaging in Living Cells

Encouraged by the above superior results of the spectral data establishing that the probe **Mito-FV** can respond to fluoride ions in acetonitrile solution, the probe **Mito-FV** seems to be useful for detecting fluoride ions in real biological samples. The standard MTT assays was carried out firstly, the result indicates that the probe **Mito-FV** at low micromolar concentrations have no marked cytotoxicity to the cells after a long period (>85% HeLa cells survived after 24 h incubation with 10 μM probe) (Fig. S6), implying that the new probe **Mito-FV** is less toxic to cells and can be used for cell imaging.

We evaluated the probe **Mito-FV** imaging fluoride ions in live cells, and the fluorescence imaging experiments were performed in living cells (HeLa cells) on confocal laser scanning microscopy. We incubated the HeLa cells with probe **Mito-FV** (10 μM) for 10 min at 37 °C under 5% CO_2 atmosphere, then washed the cells with a phosphate buffered saline (PBS) solution two times, and treated the cells with or without fluoride (100 μM) for 15 min and again washed twice with the PBS solution. When HeLa cells incubated only with **Mito-FV** for 15 min, no detectable fluorescence was observed. Contrastively, when pre-treated with **Mito-FV** for 10 min followed by the incubation of TBAF (100 μM) solution for another 15 min, strong fluorescence was observed in the blue channel (Fig. 4e; λ_{ex} = 405 nm; λ_{em} = 425–475 nm) under the same test conditions, confirming that **Mito-FV** possesses good membrane permeability and could image fluoride ions in cellular environment.

To further examine the subcellular localization of **Mito-FV**, Mito Tracker Red, the commercially available mitochondrial dye, was employed for the colocalization studies. HeLa cells were co-stained with the mitochondral tracker and **Mito-FV** in the presence of TBAF (30 μM) to performed the colocalization experiments. The merged image (Fig. 5e) showed that the staining of **Mito-FV** fits well with that of Mito Tracker Red. Moreover, the intensity profile of the linear regions of interest across HeLa cells costained with **Mito-FV** and Mito Tracker Red in the two channels varies in close synchrony (Fig. 5f). Additionally, a high overlap Pearson's colocalization coefficient (0.91) was calculated from the intensity correlation plots (Fig. 5g), indicating that the probe **Mito-FV** was localized mainly in the mitochondria and can specifically imaging the mitochondrial fluoride ions in living cells.

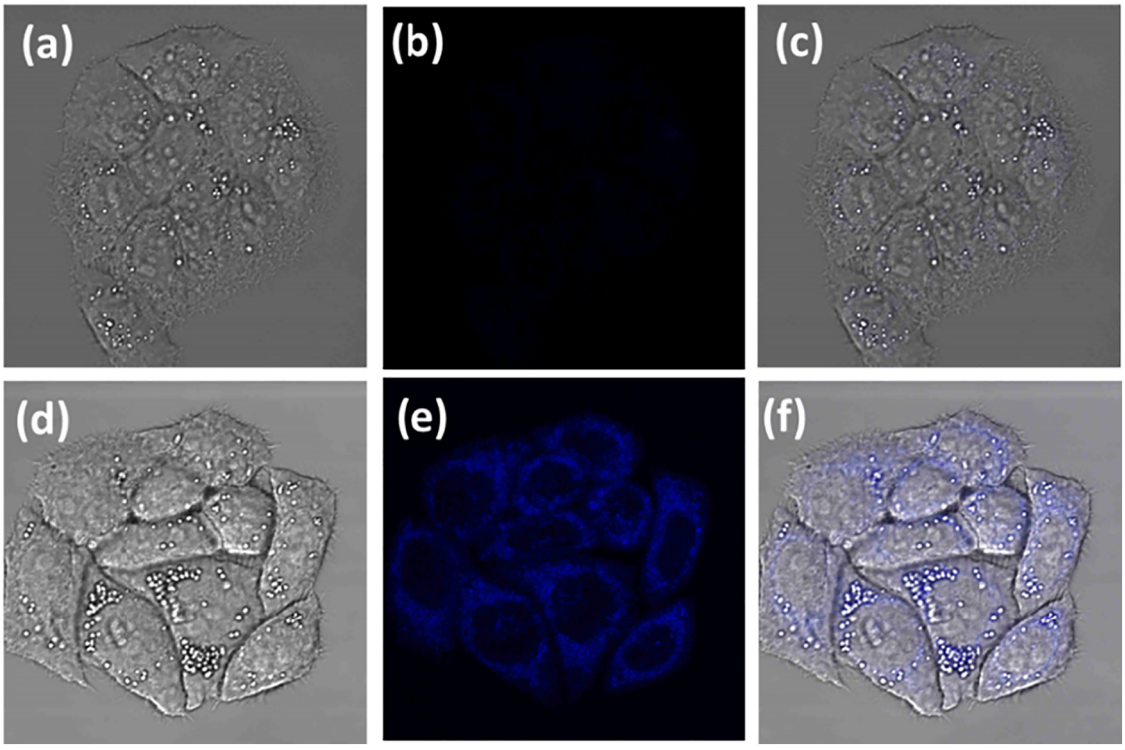

Fig. 4. Imaging of F^- in HeLa cells stained with **Mito-FV** (10 μM) (a) brightfield image of HeLa cells costained only with **Mito-FV**; (b) fluorescence images of (a) from green channel; (c) overlay of (a) and (b); (d) brightfield image of HeLa cells costained with **Mito-FV** and treated with TBAF; (e) fluorescence images of (d) from green channel; (f) overlay of (d) and (e)

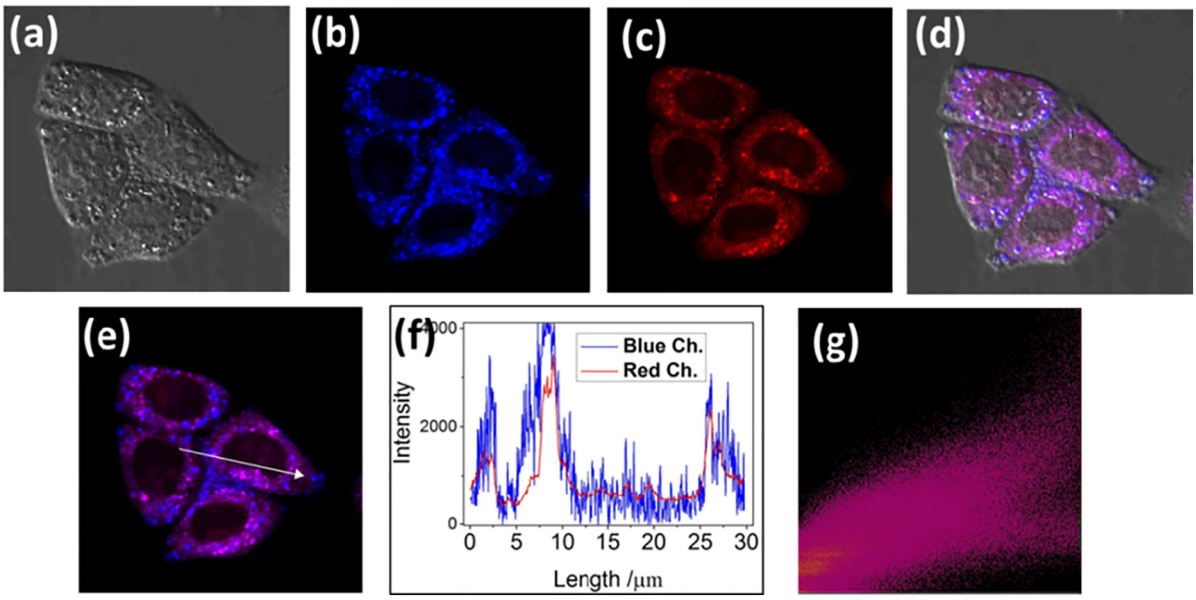

Fig. 5. Mitochondrial multicolor colocalization in HeLa cells with the probe **Mito-FV** and Mito Tracker Red. a) brightfield image; b) from blue channel (**Mito-FV** imaging of F^-); c) from the red channel (mitochondria staining); d) overlay of brighfield, blue, and red channels; e) overlay of blue and red channels; f) intensity profile of linear region of interest across the HeLa cell costained with Mito Tracker Red and blue channel of **Mito-FV**; g) intensity scatter plot of blue and red channels.

4. Conclusions

In summary, we have judiciously developed **Mito-FV**, a new fluorion probe for fluorescence cell bioimaging with a large turn-on fluorescence signal. The probe **Mito-FV** exhibited desired properties such as, high sensitivity, selectivity and fast response to fluoride ion. In addition, the compound can act as a colorimetric and stoichiometric sensor. We also demonstrated fluorescence cell bioimaging using **Mito-FV** for the detection of fluoride ions in HeLa cells under physiological conditions. The results of the cell imaging indicated that **Mito-FV** can be used to efficiently monitor the level of fluoride ions in cells, and it is worth noting that the probe was located exclusively in mitochondria.

Acknowledgement

This work was financially supported by NSFC (21472067, 21502067, 21672083), the Natural Science Foundation of Shandong Province, China (ZR2014BP001), Taishan Scholar Foundation (TS 201511041), and the startup fund of University of Jinan (309-10004, 160082101).

Appendix A. Supplementary Data

Supplementary data to this article can be found online at https://doi.org/10.1016/j.saa.2018.05.054.

References

[1] D. Jin, X. Zhao, Y. Li, X. Yan, L. Chen, A novel near-infrared colorimetric probe for fluoride anions based on a heptamethine dye, Anal. Methods 8 (2016) 6452–6457.
[2] S.Y. Kim, J.-I. Hong, Chromogenic and fluorescent chemodosimeter for detection of fluoride in aqueous solution, Org. Lett. 9 (2007) 3109–3112.
[3] J.F. Zhang, C.S. Lim, S. Bhuniya, B.R. Cho, J.S. Kim, A highly selective colorimetric and ratiometric two-photon fluorescent probe for fluoride ion detection, Org. Lett. 13 (2011) 1190–1193.
[4] W. Hu, L. Zeng, Y. Wang, Z. Liu, X. Ye, C. Li, A ratiometric two-photon fluorescent probe for fluoride ion imaging in living cells and zebrafish, Analyst 141 (2016) 5450–5455.
[5] S.Y. Kim, J. Park, M. Koh, S.B. Park, J.-I. Hong, Fluorescent probe for detection of fluoride in water and bioimaging in A549 human lung carcinoma cells, Chem. Commun. (31) (2009) 4735–4737.
[6] T.-J. Cheng, T.-M. Chen, C.-H. Chen, Y.-K. Lai, Induction of stress response and differential expression of 70 kDa stress proteins by sodium fluoride in hela and rat brain tumor 9l cells, J. Cell. Biochem. 69 (1998) 221–231.
[7] X. Shi, W. Fan, C. Fan, Z. Lu, Q. Bo, Z. Wang, C.A. Black, F. Wang, Y. Wang, A two-photon fluorescent probe for imaging aqueous fluoride ions in living cells and tissues, Dyes Pigments 140 (2017) 109–115.
[8] S.L. Edwards, T.L. Poulos, J. Kraut, The crystal structure of fluoride-inhibited cytochrome c peroxidase, J. Biol. Chem. 259 (1984) 12984–12988.
[9] P. Li, Y. Xue, W. Zhang, F. Teng, Y. Sun, T. Qu, X. Chen, X. Cheng, B. Song, W. Luo, Q. Yu, Sodium fluoride induces apoptosis in odontoblasts via a JNK-dependent mechanism, Toxicology 308 (2013) 138–145.
[10] P.M. Basha, S.M. Saumya, Suppression of mitochondrial oxidative phosphorylation and TCA enzymes in discrete brain regions of mice exposed to high fluoride: amelioration by *Panax* ginseng (Ginseng) and *Lagerstroemia speciosa* (Banaba) extracts, Cell. Mol. Neurobiol. 33 (2013) 453–464.
[11] D.A.P. Tanaka, S. Kerketta, M.A.L. Tanco, T. Yokoyama, T.M. Suzuki, Adsorption of fluoride ion on the zirconium(IV) complexes of the chelating resins functionalized with amine-N-acetate ligands, Sep. Sci. Technol. 37 (2002) 877–894.
[12] Y. Hang, C. Wu, Ion chromatography for rapid and sensitive determination of fluoride in milk after headspace single-drop microextraction with in situ generation of volatile hydrogen fluoride, Anal. Chim. Acta 661 (2010) 161–166.
[13] R.D. Marco, G. Clarke, B. Pejcic, Ion-selective electrode potentiometry in environmental analysis, Electroanalysis 19 (2007) 1987–2001.
[14] X. Yang, Y. Liu, Y. Wu, X. Ren, D. Zhang, Y. Ye, A NIR ratiometric probe for hydrazine "naked eye" detection and its imaging in living cell, Sensors Actuators B Chem. 253 (2017) 488–494.
[15] D. Li, Z. Zhong, G. Zheng, Z. Tian, A naphthalene benzimidazole-based chemosensor for the colorimetric and on-off fluorescent detection of fluoride ion, Spectrochim. Acta A 185 (2017) 173–178.
[16] B. Zhang, X. Yang, R. Zhang, Y. Liu, X. Ren, M. Xian, Y. Ye, Y. Zhao, Lysosomal-targeted two-photon fluorescent probe to sense hypochlorous acid in live cells, Anal. Chem. 89 (2017) 10384–10390.
[17] J. Li, X. Yang, D. Zhang, Y. Liu, J. Tang, Y. Li, Y. Zhao, Y. Ye, A fluorescein-based "turn-on" fluorescence probe for hypochlorous acid detection and its application in cell imaging, Sensors Actuators B Chem. 265 (2018) 84–90.
[18] A.D.S. Schramm, C.R. Nicoleti, R.I. Stock, R.S. Heying, A.J. Bortoluzzi, V.G. Machado, Anionic optical devices based on 4-(nitrostyryl)phenols for the selective detection of fluoride in acetonitrile and cyanide in water, Sensors Actuators B Chem. 240 (2017) 1036–1048.
[19] B. Dong, X. Song, X. Kong, C. Wang, Y. Tang, Y. Liu, W. Lin, Simultaneous near-infrared and two-photon in vivo imaging of H_2O_2 using a ratiometric fluorescent probe based on the unique oxidative rearrangement of oxonium, Adv. Mater. 28 (2016) 8755–8759.
[20] V. Bhalla, H. Singh, M. Kumar, Facile cyclization of terphenyl to triphenylene: a new chemodosimeter for fluoride ions, Org. Lett. 12 (2010) 628–631.
[21] N. Boens, V. Leen, W. Dehaen, Fluorescent indicators based on BODIPY, Chem. Soc. Rev. 41 (2012) 1130–1172.
[22] L. Fu, F.-L. Jiang, D. Fortin, P.D. Harvey, Y. Liu, A reaction-based chromogenic and fluorescent chemodosimeter for fluoride anions, Chem. Commun. 47 (2011) 5503–5505.

[23] J.-A. Gu, V. Mani, S.-T. Huang, Design and synthesis of ultrasensitive off-on fluoride detecting fluorescence probe via autoinductive signal amplification, Analyst 140 (2015) 346–352.
[24] N. Kumari, N. Dey, S. Bhattacharya, Rhodamine based dual probes for selective detection of mercury and fluoride ions in water using two mutually independent sensing pathways, Analyst 139 (2014) 2370–2378.
[25] B. Liu, H. Tian, A ratiometric fluorescent chemosensor for fluoride ions based on a proton transfer signaling mechanism, J. Mater. Chem. 15 (2005) 2681–2686.
[26] Q. Yang, C. Jia, Q. Chen, W. Du, Y. Wang, Q. Zhang, A NIR fluorescent probe for the detection of fluoride ions and its application in in vivo bioimaging, J. Mater. Chem. B 5 (2017) 2002–2009.
[27] X. Chen, T. Leng, C. Wang, Y. Shen, W. Zhu, A highly selective naked-eye and fluorescent probe for fluoride ion based on 1,8-naphalimide and benzothizazole, Dyes Pigments 141 (2017) 299–305.
[28] T. Gunnlaugsson, P.E. Kruger, P. Jensen, J. Tierney, H.D.P. Ali, G.M. Hussey, Colorimetric "naked eye" sensing of anions in aqueous solution, J. Organomet. Chem. 70 (2005) 10875–10878.
[29] F. Han, Y. Bao, Z. Yang, T.M. Fyles, J. Zhao, X. Peng, J. Fan, Y. Wu, S. Sun, Simple bisthiocarbono-hydrazones as sensitive, selective, colorimetric, and switch-on fluorescent chemosensors for fluoride anions, Chemistry 13 (2007) 2880–2892.
[30] Y. Wu, X. Peng, J. Fan, S. Gao, M. Tian, J. Zhao, S. Sun, Fluorescence sensing of anions based on inhibition of excited-state intramolecular proton transfer, J. Organomet. Chem. 72 (2007) 62–70.
[31] W. Xu, S. Liu, Q. Zhao, T. Ma, S. Sun, X. Zhao, W. Huang, A near-infrared phosphorescent probe for F-based on a cationic iridium(III) complex with triarylboron moieties, SCIENCE CHINA Chem. 54 (2011) 1750–1758.
[32] M. Ren, B. Deng, J.-Y. Wang, Z.-R. Liu, W. Lin, A dual-emission fluorescence-enhanced probe for imaging copper(ii) ions in lysosomes, J. Mater. Chem. B 3 (2015) 6746–6752.
[33] Y. Tan, L. Zhang, K.H. Man, R. Peltier, G. Chen, H. Zhang, L. Zhou, F. Wang, D. Ho, S.Q. Yao, Y. Hu, H. Sun, Reaction-based off-on near-infrared fluorescent probe for imaging alkaline phosphatase activity in living cells and mice, ACS Appl. Mater. Interfaces 9 (2017) 6796–6803.
[34] M. Tian, C. Wang, L. Wang, K. Luo, A. Zhao, C. Guo, Study on the synthesis and structure-effect relationship of multi-aryl imidazoles with their fluorescence properties, Luminescence 29 (2014) 540–548.
[35] D. Burtscher, R. Saf, C. Slugovc, Fluorescence-labeled olefin metathesis polymerization initiators, J. Polym. Sci. A Polym. Chem. 44 (2006) 6136–6145.
[36] K. Benelhadj, J. Massue, P. Retailleau, G. Ulrich, R. Ziessel, 2-(2′-Hydroxyphenyl) benzimidazole and 9,10-phenanthroimidazole chelates and borate complexes: solution- and solid-state emitters, Org. Lett. 15 (2013) 2918–2921.
[37] K.C. Song, H. Kim, K.M. Lee, Y.S. Lee, Y. Do, M.H. Lee, Ratiometric fluorescence sensing of fluoride ions by triarylborane–phenanthroimidazole conjugates, Sensors Actuators B Chem. 176 (2013) 850–857.
[38] L. Yuan, W. Lin, S. Zhao, W. Gao, B. Chen, L. He, S. Zhu, A unique approach to development of near-infrared fluorescent sensors for in vivo imaging, J. Am. Chem. Soc. 134 (2012) 13510–13523.
[39] M. Ren, B. Deng, X. Kong, K. Zhou, K. Liu, G. Xu, W. Lin, A TICT-based fluorescent probe for rapid and specific detection of hydrogen sulfide and its bio-imaging applications, Chem. Commun. 52 (2016) 6415–6418.
[40] S. Zhu, W. Lin, L. Yuan, Development of a near-infrared fluorescent probe for monitoring hydrazine in serum and living cells, Anal. Methods 5 (2013) 3450–3453.
[41] X. Cao, W. Lin, W. Wan, Development of a near-infrared fluorescent probe for imaging of endogenous Cu^{+} in live cells, Chem. Commun. 48 (2012) 6247–6249.
[42] Y. Chen, C. Zhu, Z. Yang, J. Chen, Y. He, Y. Jiao, W. He, L. Qiu, J. Cen, Z. Guo, A ratiometric fluorescent probe for rapid detection of hydrogen sulfide in mitochondria, Angew. Chem. Int. Ed. 52 (2013) 1688–1691.